NUMERICAL MODELING OF THREE-DIMENSIONAL FLUID FLOW WITH PHASE CHANGE

Asghar Esmaeeli, Vedat Arpacı, Department of Mechanical Engineering and Applied Mechanics, The University of Michigan, Ann Arbor, Michigan

INTRODUCTION

Bubbles are essential particles in many industrial as well as natural processes. Heat transfer through boiling, fluid cavitation, bubble driven circulation systems in metal processing, and bubble/free surface interactions in oceans are just a few examples of the many roles that bubbles play in the physical systems. One of the key questions in phase change dynamics is the prediction of mass transfer rate and its effects on the fluid flow and heat transfer of the system. There has been extensive investigations about bubble growth rate in the last few decades. The early work was concerned about solving separately the momentum and heat conduction equation and can be divided into two main categories: growth rate controlled by inertia and growth rate controlled by heat diffusion. In the inertially-controlled growth the temperature difference between bubble and liquid is negligible and the growth is controlled by the pressure difference inside and outside the bubble and inertia of the liquid. Rayleigh (1917) made such assumption to solve for the collapse of an empty cavity in a large mass of liquid. Rayleigh's solution was confined to spherically symmetric, isothermal, and inviscid flow. He also neglected the surface tension. Later on, his analysis was extended to include liquid viscosity and surface tension. In the heat diffusion controlled growth the pressure difference inside and outside bubble is negligible and the growth is controlled by heat transfer from the liquid to the bubble. The investigations of Bosnjakovic (1930), Plesset & Zwick (1952), and Skinner & Bankoff (1965) are a few examples of analyses based on the heat diffusion controlled growth. Subsequent analyses to solve the coupled equations have produced several asymptotic solutions applicable to long time only and a number of complete but approximate solutions involving simplifying assumptions about the heat conduction equation. See, for example, Plesset & Zwick (1954), Scriven (1959), and Bankoff (1958) for the former and Kosky (1968), Mikic *et al.* (1970), and Theofanous & Patel (1975) for the latter.

The use of numerical modeling in solving fluid flow with phase change is relatively new. One of the earliest of such studies is the potential flow solution of Plesset & Chapman (1971) for the collapse of an isothermal spherical vapor bubble in the neighborhood of a solid wall. A number of authors have tried to solve the boiling bubble problem by coupling the momentum equation with a simplified form of the energy equation. See Theofanous *et al.* (1969) and Prosperetti & Plesset (1977), for example. Dalle Donne & Ferranti (1975) were among the first to solve the complete equations of motion and energy. More recent numerical studies about boiling bubbles include boundary fitted/finite element method of Schunk & Rao (1994), finite volume/moving mesh method of Welch (1995), level set method of Son & Dhir (1997), and front tracking/finite difference technique of Juric & Tryggvason (1995).

So far, the last two studies present the most comprehensive numerical modeling of the phase change problem leaving aside their two-dimensionality. While it is possible to predict some of the qualitative features of the phase change phenomena by two-dimensional simulations, it is generally believed that these computations fail to provide an accurate account of the quantitative features. Therefore, it is necessary to relax this restriction in order to obtain a more realistic picture of the problem. Our aim is to present a numerical technique for modeling three-dimensional fluid flow with phase change. To the best of our knowledge, this is the first numerical study that addresses this issue. In an earlier study (i.e. Esmaeeli & Arpacı, 1998), we used a similar methodology to simulate phase change without fluid flow.

FORMULATION AND NUMERICAL METHOD

Consider a domain consisting of a liquid and its vapor undergoing phase change. The material properties of the fluids are different but constant within each phase. The governing equations for this problem are conservation of mass, momentum, and energy equations within each phase, and the jump conditions across the interface. Rather than writing the governing equations separately for each of the fluids, a single set of equations are used which are valid for the entire flow field and take the jump in properties across the interface into account. The momentum equation in conservative form for such a flow is:

$$\frac{\partial \rho \overline{u}}{\partial t} + \nabla \cdot \rho \overline{u}\,\overline{u} = -\nabla p + \nabla \cdot \mu(\nabla \overline{u} + \nabla \overline{u}^T) - \rho \overline{g} + \oint \sigma \kappa \overline{n} \delta(\overline{x} - \overline{x}^f) dA. \quad (1)$$

In the above equation $\overline{u}$ is the velocity, p is the pressure, ρ is the density, μ is the viscosity, $\overline{g}$ is the gravity, σ is the surface tension coefficient, κ is twice the mean curvature, and $\overline{n}$ is the unit vector normal to the interface. $\delta(\overline{x} - \overline{x}^f)$ is a delta function which is zero everywhere except at the interface where $\overline{x} = \overline{x}^f$ and dA is differential area of the interface.

The energy equation in conservative form is:

$$\frac{\partial \rho c T}{\partial t} + \nabla \cdot \rho c \overline{u} T = \nabla \cdot k \nabla T + \oint \overline{h} \rho_f (\overline{u}_i - \overline{u}_f).\overline{n} \delta(\overline{x} - \overline{x}^f) dA, \quad (2)$$

where T is the temperature, c is the heat capacity, and k is the heat conductivity. The last term in the above equation acts as a heat source (sink) which is zero away from the interface and its inclusion enforces the conventional energy jump condition across the front. Here, ρ_f and $\overline{u}_f$ are the fluid density and velocity at the liquid or vapor side of the interface, and $\overline{u}_i$ is the interface velocity. $\overline{h}$ is a measure of difference in the enthalpies of the liquid and the vapor and is derived using thermodynamics consideration:

$$\overline{h} = h_{fg} + T_{eq}(c_l - c_v). \quad (3)$$

Here, h_{fg} is the latent heat of evaporation, T_{eq} is the equilibrium temperature, and c_l and c_v are the heat capacities of the liquid and the vapor, respectively.

The mass conservation is:

$$\nabla \cdot \rho \overline{u} = \oint (\rho_v - \rho_l) u_n \delta(\overline{x} - \overline{x}^f) dA, \quad (4)$$

where, $u_n = \overline{u}_i.\overline{n}$. The above equation is equivalent to the conventional mass conservation equation but is better suited for numerical formulation.

The introduction of the interface velocity $\overline{u}_i$ adds an additional unknown to the problem. This new unknown is being taken care of by implementation of the modified Gibbs-Thomson relation at the interface:

$$T_f = T_{eq} + \frac{\sigma \kappa T_{eq}}{\rho_f h_{fg}} + \frac{(c_l - c_v)}{h_{fg}}(T_f - T_{eq})^2 - \frac{\rho_f (\overline{u}_i - \overline{u}_f) \cdot \overline{n}}{\phi}, \quad (5)$$

where ϕ is the kinetic mobility. The above equation was first derived by Alexiades & Solomon (1993) and then modified by Juric & Tryggvason (1996) to include the kinetic mobility effect.

The above equations are supplemented by the equations of state for the material properties:

$$\frac{\mathcal{D}\rho}{\mathcal{D}t} = 0; \quad \frac{\mathcal{D}\mu}{\mathcal{D}t} = 0; \quad \frac{\mathcal{D}k}{\mathcal{D}t} = 0; \quad \frac{\mathcal{D}c}{\mathcal{D}t} = 0, \quad (6)$$

where

$$\frac{\mathcal{D}}{\mathcal{D}t} = \frac{\partial}{\partial t} + \overline{u}_i \cdot \nabla. \quad (7)$$

Our numerical technique is an extension to the two-dimensional model developed by Juric & Tryggvason (1995). Extension of the method to three dimensions involves a number of complications in the operations on the front which will be addressed in a future publication. We use a fixed (i.e. Eulerian), regular, and staggered grid to discretize the governing equation and an unstructured (i.e. Lagrangian) grid to represent the front and to construct the material property fields. This unstructured grid is also used to distribute the source terms in the right hand side of mass conservation, momentum, and energy equations to the Eulerian grid and to interpolate the velocity, temperature, and density at the front points from the grid.

The computations start with construction of the initial temperature field T^n and the material property fields ρ^n, μ^n, c^n, k^n using known position of the front at $t = 0$, where $n = 1$. The front is then moved to a new position using the interface velocity at the current time $\overline{u}_i{}^n$. The surface tension is distributed to the grid as a body force using Peskin distribution function (see Peskin 1977) and the density ρ^{n+1} and heat capacity c^{n+1} fields are constructed at the new position. A modified projection algorithm which is first order in time and second order in spatial dimensions is used to solve the momentum equation. In the absence of pressure term, the momentum equation is solved and a provisional (i.e. unprojected) velocity field $\overline{u^*}$ is computed. The iterative part starts by guessing the front velocity at the next time step and construction of the mass source at the new position of the front. An elliptic pressure equation is then solved and the provisional velocity is corrected for the pressure to obtain the projected velocity $\overline{u}^{n+1}$. The velocity of the fluid at the front position $\overline{u}_f{}^{n+1}$ is interpolated using a Peskin interpolation function (see Peskin 1977) and the heat source is constructed. The energy equation is then solved for T^{n+1} and the Gibbs-Thomson relation is checked at the front points. If this equation is satisfied for all the front points within a predetermined tolerance, the heat conduction coefficient k^{n+1} and viscosity fields μ^{n+1} are updated for the next time step and the calculation proceeds. Otherwise, a new guess is proposed for the front velocity and the computations are repeated.

The individual parameters that control the problem are ρ_l, ρ_v, μ_l, μ_v, k_l, k_v, c_l, c_v, h_{fg}, g, ϕ, σ, $T_\infty - T_{eq}$, and initial diameter of the bubble, d_0. Here, T_∞ is the initial temperature of the fluid outside the bubble. Nondimensionalization results the following parameters: ρ_v/ρ_l, μ_v/μ_l, k_v/k_l, c_v/c_l, $Ja = c_l(T_\infty - T_{eq})/h_{fg}$, $Pr = \mu_l c_l/k_l$, $Gr = \rho_l g(\rho_l - \rho_v)d_0{}^3/\mu_l{}^2$, $Ca = c_l(T_\infty - T_{eq})\sigma/\rho_l h_{fg}{}^2 d_0$, and $\vartheta = k_l/\phi\rho_l h_{fg} d_0$. Ja is the Jacob number which is ratio of the sensible to the latent heat, Pr is the Prandtl number which is a measure of diffusion of momentum with respect to thermal energy, Gr has a strong resemblance to the Grashof number, Ca is a capillary number which is ratio of surface tension to viscous force, and ϑ is nondimensional kinetic mobility. When we present our results, $l_s = d_0$, $u_s = \mu_l/\rho_l d_0$, and $t_s = l_s/u_s$ are used as length, velocity, and time scales.

RESULTS

Here, we present some preliminary results using our numerical technique. We are interested in growth of a bubble in a superheated liquid. The growth of a vapor bubble in a superheated liquid is controlled by three factors: liquid inertia, surface tension, and heat diffusion. These factors determine what is called "the critical radius" which is the minimum radius that a nucleus should start with in order to grow. In the current study, we choose the initial bubble radius considerably larger than the critical radius. Therefore, we expect the bubble to grow.

We start our analysis by considering the behavior of a single bubble in zero gravity. The first frame of figure (1) shows the initial position of the bubble in a domain. The domain size (nondimensionalized by dividing by bubble diameter) is $2.5 \times 2.5 \times 5$ and the grid resolution is $48 \times 48 \times 96$. The initial front consists of 5832 triangular elements. Initially the liquid is superheated, the vapor is at the equilibrium temperature, and the flow is quiescent. The nondimensional variables are $Ja = 0.1$, $Pr = 0.25$, $Ca = 0.02$, and $\vartheta = 0.01$. The ratio of material properties are $\rho_v/\rho_l = 0.1$, $\mu_v/\mu_l = 0.05$, $k_v/k_l = 0.025$, and $c_v/c_l = 1.0$. The domain is periodic in the horizontal direction, wall-bounded (and insulated) at the bottom, and open at the top. At the top boundary, the pressure and normal gradient of velocity and temperature are set to zero. The second frame shows the bubble and a normal section of velocity field at the middle of the domain at time $t = 0.053$. The bubble elongates in the vertical direction. Since the gravity is zero, there is no vortical structure inside the bubble. The velocity field in the vicinity of the bubble is relatively disturbed but it is uniform in the rest of the domain. The liquid exits from the top boundary due to fluid expansion at the interface. The fluid velocity is higher around the top of the bubble compared to its side. This is due to the constrain imposed on the flow by periodicity in the horizontal direction and the existence of the wall at the bottom. This results in a higher evaporation rate around the top portion of the bubble and consequently the bubble deforms to an egg-like shape (third frame, $t = 0.106$). The ratio of final volume of the bubble to its initial volume is about fifteen. At the end of the simulation, the bubble consists of 45704 triangular elements.

In the next simulation we study growth of a bubble under high gravity. The initial setup is the same as the previous simulation. The nondimensional numbers for this run are $Ja = 0.1$, $Pr = 0.25$, $Gr = 0.32 \times 10^3$, $Ca = 0.004$, and $\vartheta = 0.05$. With the exception of density ratio which is increased to $\rho_v/\rho_l = 0.5$, all the other material property ratios are the same as the corresponding ones in the first simulation. The grid resolution is the same as the previous run. Lower density difference results in a smaller front velocity which compensates for the higher resolution that may be needed to accurately resolve this case. The first frame of figure 2 shows the bubble and the velocity field at $t = 0.0875$. The velocity is higher inside the bubble due to buoyancy. Two counter rotating vortices appear on the side of bubble which pump hot fluid from the top to the rear. Since the bubble grows, we expect the rise velocity to increase as a result of enhanced buoyancy. This is indeed the case as is seen from the scale of the velocities in the second frame at $t = 0.22$. The evaporation rate is more uniform compared to the previous case. This is due to the fact that the side of the bubble now has a chance to receive hot fluid as the bubble moves upward. As a result, the elongation in the vertical direction is much smaller compared to the first case. Moreover, unlike the previous run, an indentation appears at the rear of the bubble. This is a hydrodynamic effect and is formed as a result of local competition between the surface tension, pressure, and viscous forces. This indentation is increased as the bubble rises (third frame, $t = 0.268$). Although the high curvature developed at the rim of the bubble is a challenge to accurate computation of surface tension, comparison of our results with curvatures of analytical surfaces showed that our method successfully resolves this issue.

Inspection of the temperature field for both cases (not shown in the text) showed the gradual depletion of the superheat. The initial sharp temperature gradient at the interface was replaced with a less steep temperature gradient as a result of heat diffusion. This did not have a pronounced effect at the early period of growth. However, it decreased the growth rate at the later time.

CONCLUSIONS

We have used direct numerical simulation to study phase change phenomena. Numerical simulation of a three-dimensional boiling bubble in zero gravity showed the deformation of the bubble to an egg-like shape as a result of nonuniform evaporation at the phase boundary. Similar computations for a bubble under high gravity showed the formation of a "dimpled" bubble. For both cases, the growth rate started to halt as a result of depletion of the superheat.

ACKNOWLEDGMENT

This work was supported by NASA Microgravity program under contract number NAG3-1952 with Dr. An-Ti Chai as principal investigator. We would like to acknowledge helpful discussions with Dr. Chai during the course of this study and assistance of Dr. Amadi Nwankpa in using visualization software.

REFERENCES

Alexiades, V., and Solomon, A. D., 1993, "Mathematical

modeling of melting and freezing processes," Hemisphere, Washington, D. C., pp. 92-94.

Bankoff, S. G., 1963, "Asymptotic growth of a bubble in a liquid with uniform initial superheat," Appl. Sci. Res. sect. A, Vol. 12, pp. 267-281.

Bosnjakovic, F., 1930, Tech. Mech. Thermodynamics, Vol. 1, 358.

Dalle Donne, M., and Ferranti, M. P., 1975, "The growth of vapor bubble in superheated sodium," Int. J. Heat Mass Transfer, Vol. 18, pp. 477-493.

Esmaeeli, A., and Arpacı, V., 1998, "Numerical modeling of three-dimensional dendritic solidification," paper number FEDSM98-4983, ASME proceedings of the 1998 ASME-FED summer meeting, June 21-25, 1998, Washington, D.C., Editor: D. O. Davis.

Florschuetz, L. W., Henry, C. L., and Rashid Khan, A., 1969, "Growth rates of free vapor bubbles in liquids at uniform superheats under normal and zero gravity conditions," Int. J. Heat Mass Transfer, Vol. 12, pp. 1465-1489.

Forster, H. K., and Zuber, N., 1954, "Growth of a vapor bubble in a superheated liquid," J. Appl. Phys., Vol. 25, pp. 474-478.

Forster, H. K., and Zuber, N., 1955, "Dynamics of vapor bubble and boiling heat transfer," A.I.Ch.E. Journal, Vol. 1, pp. 531-535.

Juric, D., and Tryggvason, G., 1995, "A front-tracking method for liquid-vapor phase change," FED-Vol. 234, pp. 141-148. ASME Winter Annual Meeting, San Francisco, CA, Nov. 12-17, 1995.

Juric, D., and Tryggvason, G., 1996, "Direct numerical simulations of flows with phase change," AIAA 96- 0857, 34th AIAA Aerospace Sciences Meeting, Reno, NV, Jan. 15-18, 1996.

Kosky, P. G., 1968, "Bubble growth measurements in uniformly superheated liquids," Chem. Engng. Sci., Vol. 23, pp. 695-703.

Mikic, B. B., Rohsenow, W. M., and Griffith, P., 1970, "On bubble growth rates," Int. J. Heat Mass Transfer, Vol. 13, pp. 657-666.

Peskin, C. S., 1977, "Numerical analysis of blood flow in the heart," J. Comput. Phys., Vol. 25, pp. 220-252.

Plesset, M. S., and Chapman, R. B., 1971, "Collapse of an initially spherical vapor cavity in the neighborhood of a solid boundary," J. Fluid Mech., Vol. 47, pp. 283-290.

Plesset, M. S., and Zwick, S. A., 1952, "A nonsteady heat diffusion problem with spherical symmetry," J. Appl. Phys., Vol. 23, pp. 95-98.

Plesset, M. S., and Zwick, S. A., 1954, "The growth of vapor bubbles in superheated liquids," J. Appl. Phys., Vol. 25, pp. 493-500.

Plesset, M. S., and Prosperetti, A., 1977, "Bubble dynamics and cavitation," Ann. Rev. Fluid Mech., Vol. 9, pp. 145-181.

Prosperetti, A., and Plesset, M., 1978, "Vapor-bubble growth in a superheated liquid," J. Fluid Mech., Vol. 85, pp. 349-368.

Rayleigh, L., 1917, "On the pressure developed in a liquid during the collapse of a spherical cavity," phil. Mag., Vol. 34, pp. 94-98.

Schunk, P. R., and Rao, R. R., 1994, "Finite element analysis of multicomponent two-phase flows with interphase mass and momentum transport," Int. J. Num. Meth. Fluids, Vol. 18, pp. 821-842.

Scriven, L. E., 1959, "On the dynamics of phase growth," Chem. Engng. Sci., Vol. 10., pp. 1-13.

Skinner, L. A. and Bankoff, S. G. Dynamics of vapor bubbles in general temperature fields. Physics of Fluids Vol. 8, pp. 1417-1420.

Son, G., and Dhir, V. K., 1997, "Numerical simulation of saturated film boiling on a horizontal surface," J. Heat Transfer, pp. 525-533.

Theofanous, T. G., and Patel, P. D., 1975, "Universal relations for bubble growth," Int. J. Heat Mass Transfer, Vol. 199, pp. 425-429.

Theofanous, T. G., Biasi, L., and Isbin, H. S., 1969, "A theoretical study on bubble growth in constant and time-dependent pressure fields," Chem. Engng. Sci., Vol. 26, pp. 263-274.

Welch, S. W. J., 1995, "Local simulation of two-phase flows including interface tracking with mass transfer," J. Comp. Phys., Vol. 121, pp. 142-154.

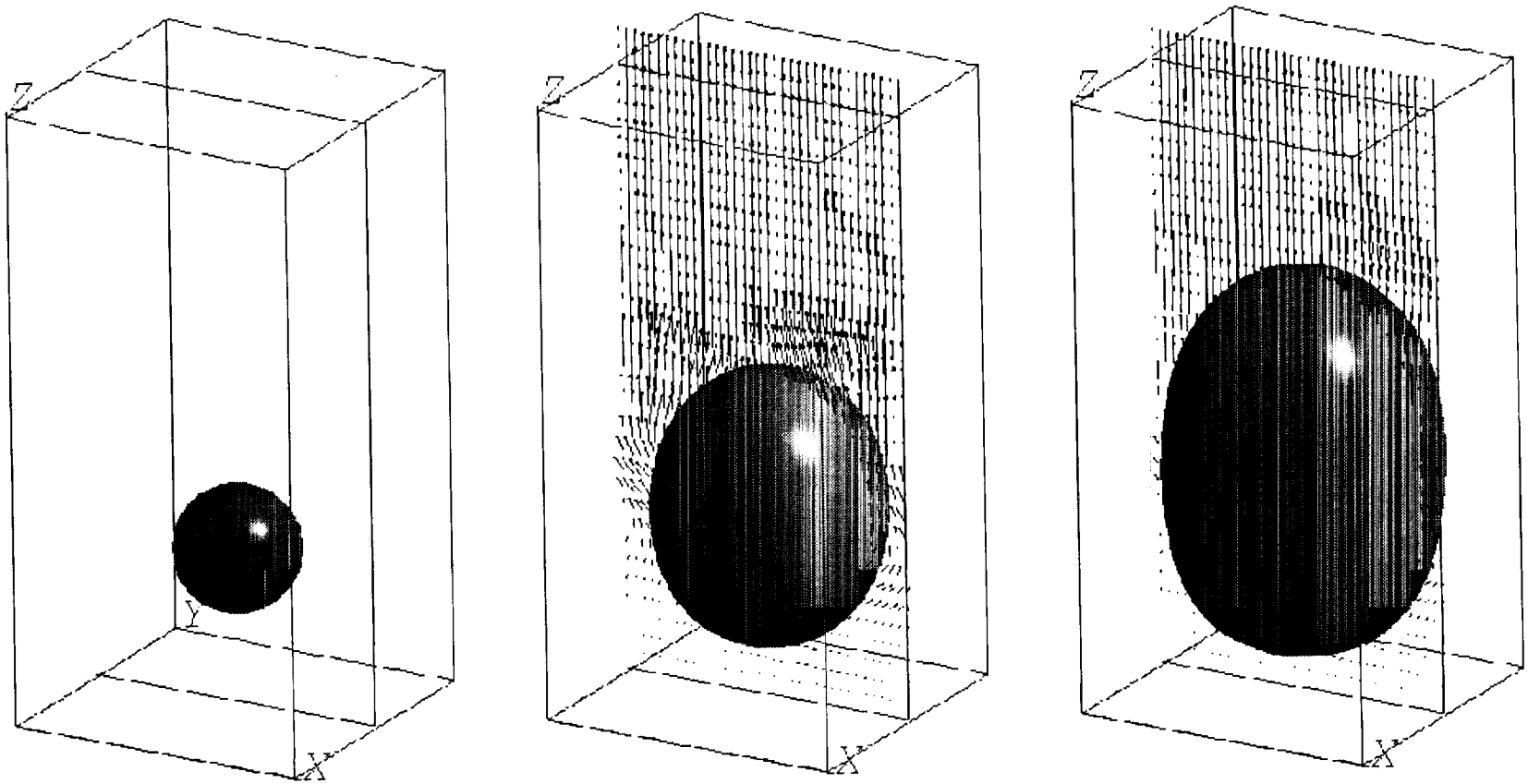

Figure 1. Growth of a vapor bubble in a superheated liquid under zero gravity. Here, $Ja = 0.1$, $Pr = 0.25$, $Ca = 0.02$, and $\vartheta = 0.01$. The ratio of material properties are $\rho_v/\rho_l = 0.1$, $\mu_v/\mu_l = 0.05$, $k_v/k_l = 0.025$, and $c_v/c_l = 1.0$.

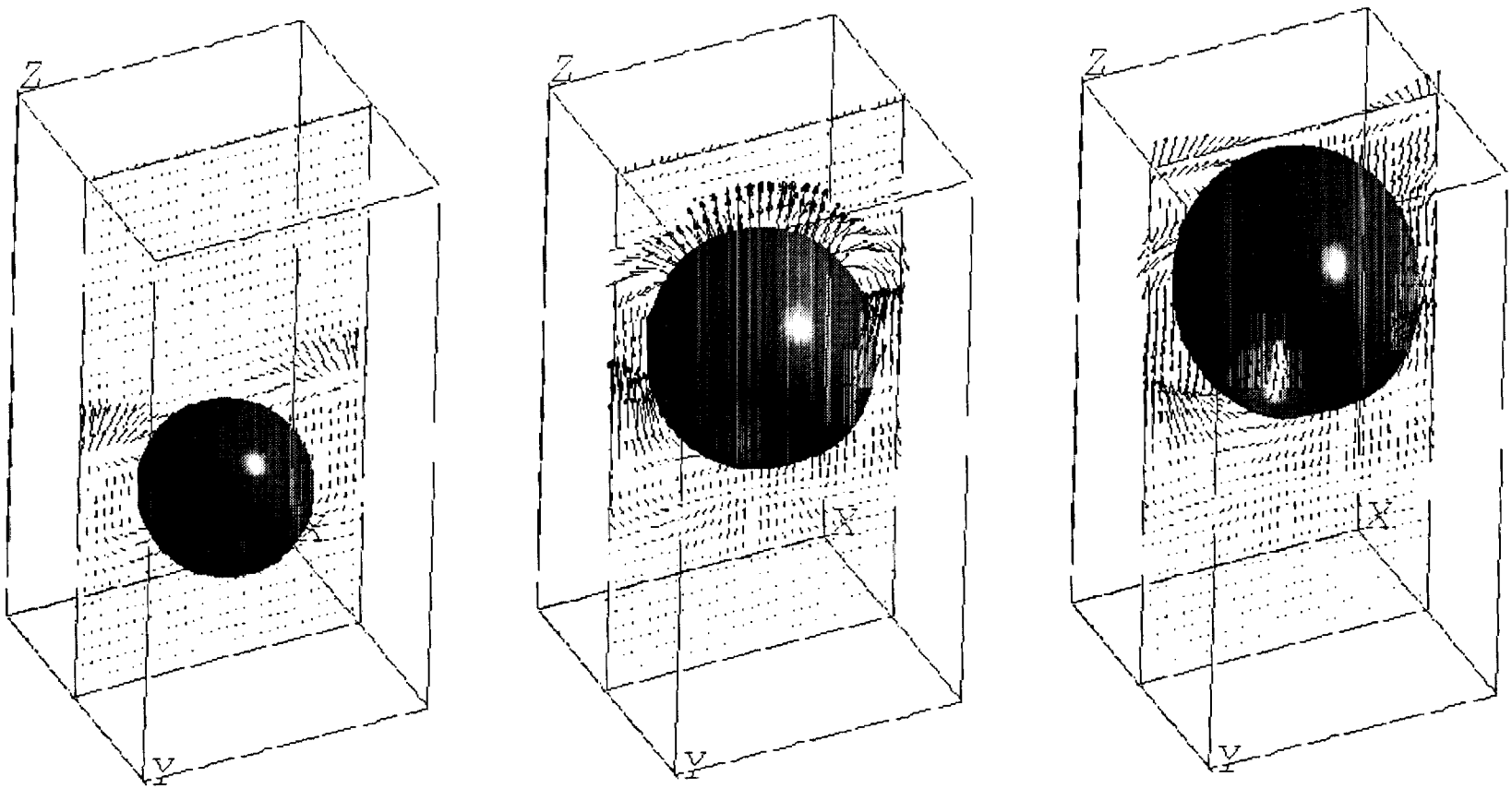

Figure 2. Growth of a vapor bubble in a superheated liquid under high gravity. Here, $Ja = 0.1$, $Pr = 0.25$, $Gr = 0.32 \times 10^3$, $Ca = 0.004$, and $\vartheta = 0.05$. The ratio of material properties are $\rho_v/\rho_l = 0.5$, $\mu_v/\mu_l = 0.05$, $k_v/k_l = 0.025$, and $c_v/c_l = 1.0$.